Article Type: **Research Article**

Article Category: **Sports Coaching**

Tittle: **Experimental and Numerical Study of the Flow past Olympic Class K-1 Flat Water Racing Kayak at Steady Speed**

Running Head: **Flat Water Racing Kayak Resistance Study**

Authors: **Georgios D. Tzabiras, Stylianos P. Polyzos, Konstantina Sfakianaki, Basilios Diafas, Athanasios D. Villiotis, Konstantinos Chrisikopoulos and Sokrates Kaloupsis**

Corresponding Author:

Stylianos Polyzos, Mr

Laboratory for Ship and Marine Hydrodynamics,

9 Heroon Polytechniou str. NTUA Campus, Zografos 15773, Greece

spolyzos@mail.ntua.gr

0030-2107721104

George Tzabiras is a Professor and Head of the Laboratory for Ship and Marine Hydrodynamics of the National Technical University of Athens (NTUA).

Stylianos Polyzos and Konstantina Sfakianaki are Phd Candidates at the Laboratory for Ship and Marine Hydrodynamics.

Basilios Diafas, Athanasios D. Villiotis, Konstantinos Chrisikopoulos and Sokrates Kaloupsis, are members of the Pan-Hellenic Kayak and Canoe Trainers Association and the University of Athens, Faculty of Physical Education and Sport Science.

Experimental and Numerical Study of the Flow past Olympic Class K-1 Flat Water Racing Kayak at Steady Speed

ABSTRACT

The present work is concerned with the study of the hydrodynamic performance of an Olympic class “K-1”flat water racing Kayak. Experiments in calm water and regular waves were conducted at the towing tank of the Laboratory for Ship and Marine Hydrodynamics (LSMH) of NTUA. Furthermore, systematic numerical tests using both Potential and RANS solvers have been performed in order to investigate whether CFD tools can be applied for predicting the calm water resistance of similar vessels under the scope of hull optimization. The numerical results are in good agreement with the experiments thus forming a basis for further investigation and deeper understanding of the athlete-boat interaction, especially for high performance and high competitive boats.

Key words: racing-kayak, resistance, experiments, potential, RANS

INTRODUCTION

The scope of the present work is to investigate the hydrodynamic behavior of an Olympic class K-1 Flat Water Racing Kayak boat at steady forward speed. In a first approximation, the complicated roll and yaw motion of the boat caused by the rower is simplified by regarding only the forward component including free heave and trim. The athlete is in any case replaced by a constant weight about his/her mean centre of gravity. The study includes both experimental and numerical tests. Basically, the aim of the experimental program was to measure the total resistance of the Kayak, covering a speed range of 0.25 to 5.15 m/s, at the towing tank of the Laboratory for Ship and Marine Hydrodynamics (LSMH) of NTUA. The experiments were carried out in calm water and low regular waves. The tests took place during the last week of January 2009. In addition, numerical experiments were also performed using both a non-linear potential flow solver as well as a Reynold's Averaged Navier-Stokes (RANS) solver, in order to explore the validity of CFD (Computational Fluid Dynamics) in predicting the basic flow features past the examined vessel.

METHODS

Experimental method

All the experiments were performed in the towing tank of the LMSH. The dimensions of the towing tank are 91 m (effective length), 4.56 m (width), and 3.00 m (depth). The towing tank is equipped with a running carriage that can achieve a maximum speed of 5.2 m/s. The tank is also equipped with a wave generating paddle (wave maker), located at the one end of the flume. At the opposite end there is a properly shaped inclined shore, for the absorption of the waves. The wave making facilities can produce both harmonic and pseudorandom waves, in the frequency range from 0.3 to 1.4 Hz. The corresponding significant wave height can reach the level of 25 cm.

The hull provided by Pan-Hellenic Kayak and Canoe Trainers Association (PA.SY.P.K-C) was an Olympic class flat water racing Kayak, K-1 category, which refers to a single-seat

boat, having the athlete paddling in a seated position. The weight category of the boat is M (medium), corresponding to an athlete's weight in the range of 70 to 80 Kgr.

Minor alterations on the internal structure of the model were applied prior to the measurements, in order to accommodate the measuring equipments. This work was supervised by the personnel of PA.SY.P.K-C.

Both experimental and numerical tests were carried out with the boat having a displacement of Δ=86.8 kg (condition A). This is the sum of the bare hull weight with the added fixtures (11.8 Kg) and the mean athlete's weight, the last taken as 75 Kg for the present study. The longitudinal position of the center of gravity (LCG) was chosen at the middle of the athlete's seat. For the experiments, the rod of the resistance dynamometer was mounted on the hull at this location. The mounting was done using a heave rod - pitch bearing assembly, which allows the vertical motions and trim angles (heave and pitch responses) of the boat.

The resistance measurements were performed for speeds in the range from 0.25 to 5.15 m/s, for the case of calm water and for two speeds (2.5 and 5.0 m/s) for the case of harmonic waves, (3). All the tests were performed in fresh water.

The boat resistance, the rise of the center of gravity (CG rise), the dynamic trim and the towing speed of the model were recorded during the runs on calm water. In addition, for the case of harmonic waves, the wave elevation was measured using wave probes.

Numerical methods

In order to investigate whether CFD tools can be applied with confidence to predict the calm water resistance of similar vessels under the scope of hull optimization, systematic numerical tests were carried out by applying the non-linear potential flow solver (5,6), as well as the RANS solver (4,6), both developed at LSMH.

The potential method is based on source quadrilateral panels that cover the wetted surface of the boat and the real free-surface (Figure 1). The latter is found by an iterative procedure

which, after convergence, leads to the satisfaction of both the well known free surface conditions: the kinematic and the dynamic. The potential flow predicts the wave making component C_W, whereas the total resistance coefficient C_F is calculated by adding the corresponding 1957 International Towing Tank Conference (ITTC'57) skin friction value.

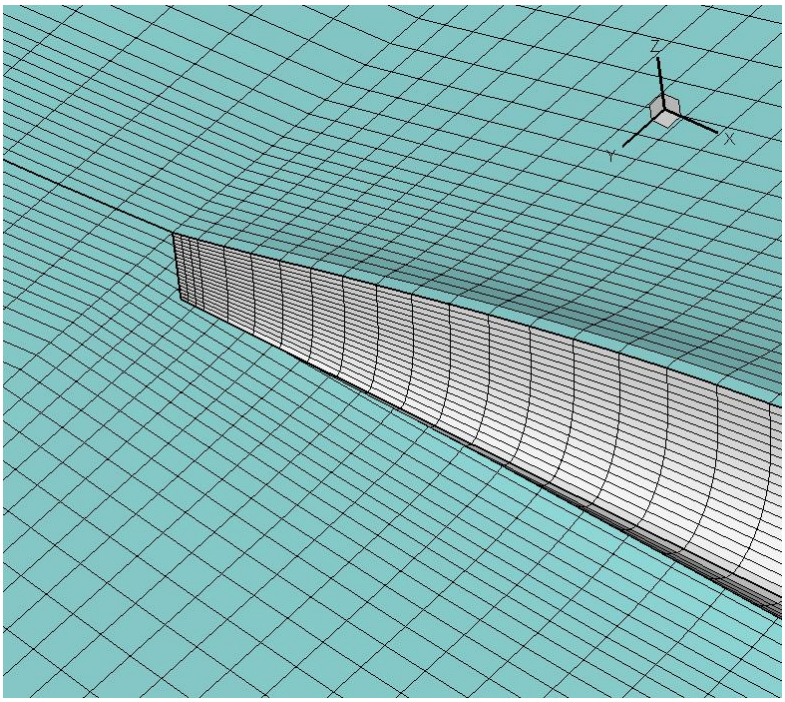

Figure 1 Panels on the hull and water surface.

Naturally, this procedure suffers from the potential flow drawbacks, i.e. the predicted wave pattern near and after the stern does not include any viscous effects. Besides, the so called form-resistance component including the skin friction alteration due to the shape of the hull and the viscous pressure component cannot be taken into account. These shortcomings disappear when the RANS equations are solved numerically. The latter, however, require substantially higher computing power and time since a three-dimensional grid discretisation is required, Figure 2.

The employed method uses an H-O type numerical grid which is adjusted to the free-surface as the solution proceeds (4). To account for turbulence effects, the well known k-ε model with wall functions (1) has been adopted.

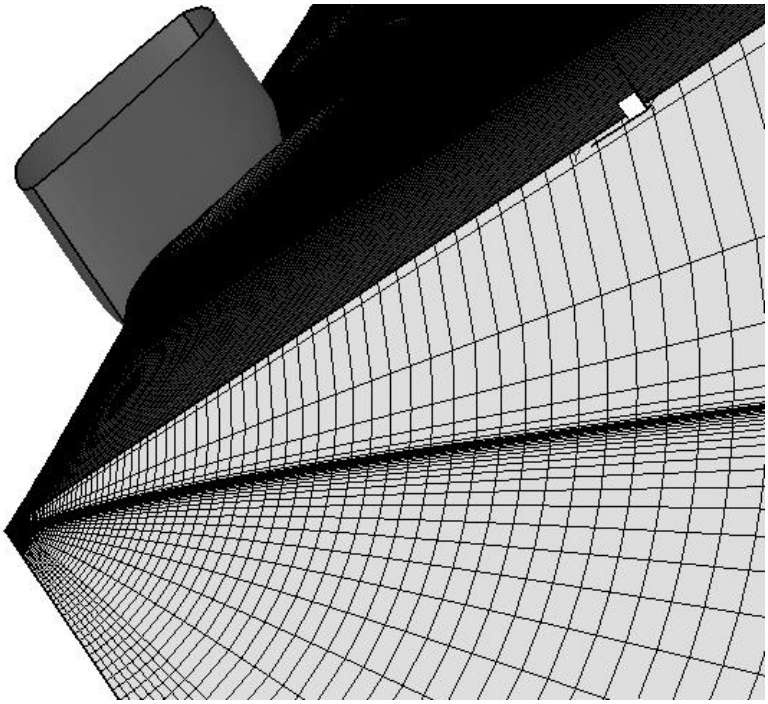

Figure 2 RANS numerical grid

RESULTS

Calm water experiments

As aforementioned, the calm water resistance tests were done for the speed range of 0.25 to 5.15 m/s. The experimental results concerning the calm water resistance, the CG rise, the dynamic trim and the towing speed of the Kayak are presented in Table 1. Besides, the corresponding graphs for the resistance, dynamic trim and CG rise are presented in Figs. 3 to 5, respectively.

As observed in Fig. 4, the dynamic trim is negligible in the range of speeds 0-2.5 m/s while it increases rapidly after it resulting to an increase of the draft at the stern and a raise of the

bow. The CG –rise, Fig. 5, is always negative resulting to an increase of the mean vessels draft which presents a peak about the speed of 3.5 m/s. This behavior could be associated with the dynamic trim change and shows that the behavior of the boat is very sensitive with respect to the speed.

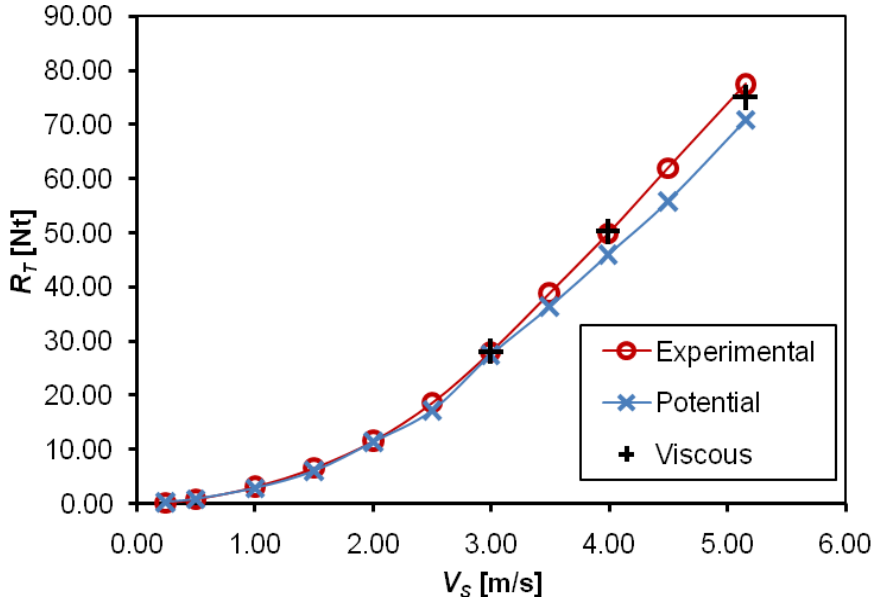

Figure 3 Total Resistance.

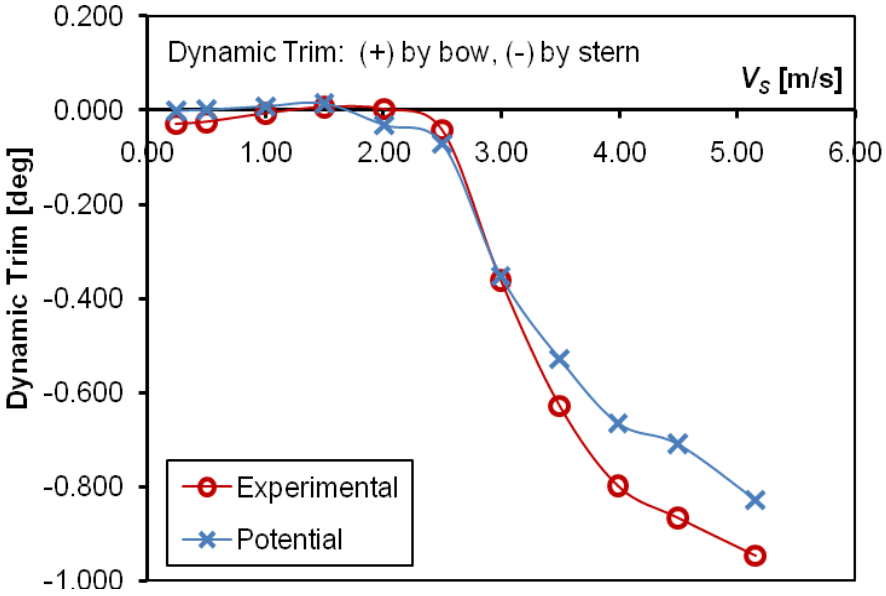

Figure 4 Dynamic Trim.

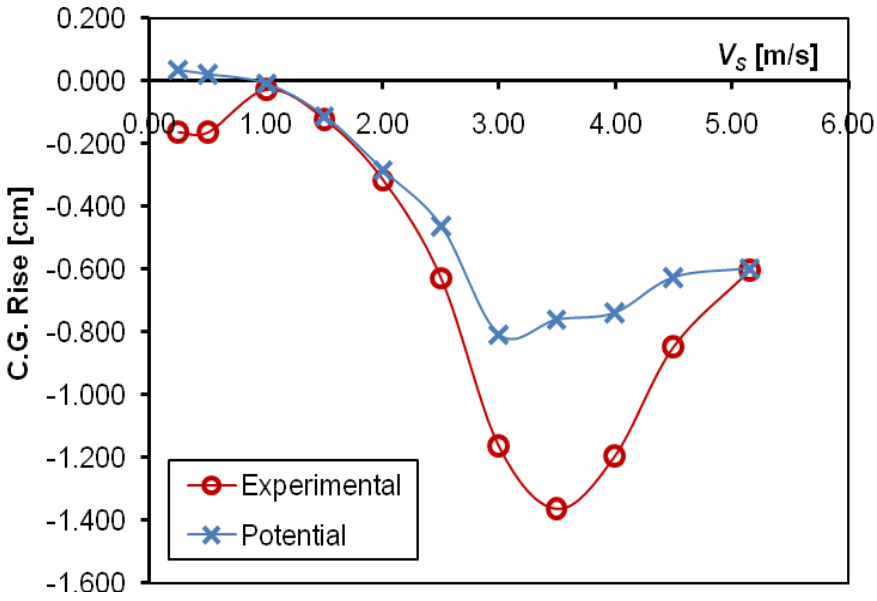

Figure 5 C.G. Rise.

In order to study the usual Froude decomposition of the total resistance coefficient versus speed, the relation between the total resistance coefficient (C_T) and the Froude number (Fn) is, firstly, depicted in Figure 6. These parameters are defined by the following relations:

$$Fn = \frac{V_S}{\sqrt{g \cdot L}}$$

$$C_T = \frac{R_T}{\left(\frac{1}{2} \cdot \rho \cdot WS \cdot V_S^2\right)}$$

where V_S stands for the speed, g is the gravitational acceleration, L the waterline length, R_T the total resistance, ρ the water density and WS the wetted surface.

In the calculation of the total resistance coefficient, the wetted surface used, was the one calculated by means of the potential method. The variation total resistance coefficient vs. Fn, presented in Fig.6, shows that it is influenced strongly by the wave formation. The main hump is located in the region of Fn 0.4÷0.45, i.e. it is moved to the left with respect to the predicted one by the linear wave theory (about 0.5) (2). Besides, the prismatic hump is missing while a "hollow" appears about Fn=0.3 which is moved to the right with respect to the predicted one by

the linear wave theory (about 0.24), while the higher values at the low Fn show a dominant effect of skin friction.

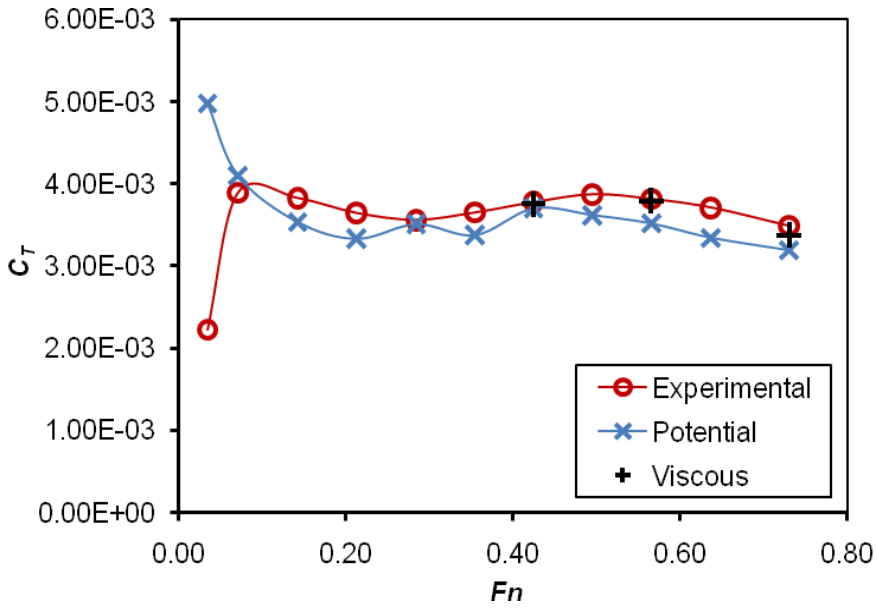

Figure 6 Total resistance coefficient.

According to the standard Froude approach, the total resistance coefficient can be decomposed into the friction (C_F) and the residual (C_R) components as:

$$C_T = C_F + C_R$$

The friction coefficient (C_F) can be calculated by the ITTC'57 formula as:

$$C_F = \frac{0.075}{(\log_{10} Rn - 2)^2}$$

where $Rn = \frac{V_S \cdot L}{\nu}$ represents the corresponding Reynolds number, L is the immersed waterline length and ν the kinematic viscosity

Furthermore, the residual resistance may be regarded as equal to the so called wave-making resistance C_W, i.e. $C_R \approx C_W$. The three coefficients with respect to the Froude number are presented in Table 2. The negative or very low values of C_R at the lower Froude numbers show that the skin friction formula rather over-predicts C_F and, therefore, an extended laminar region

may cover the front part of the vessel. It should be noted here, that no turbulence stimulators were applied since the real hull was tested. The slender form of this hull should result to a thin boundary layer region over the major part of the wetted surface, thus permitting the existence of a laminar zone especially at low speeds, which in any case is favorable because it leads to a reduction of the total resistance.

The residual resistance coefficient, plotted vs. Fn in Fig. 7, shows similar trends with Fig. 6 and influences accordingly the total coefficient. C_R is comparable to C_F after Fn=0.3, but in any case is lower than that, implying that skin friction plays an important role for the total resistance. This trend is due to the very slender form of the particular boat which has been designed to produce as far as possible low waves.

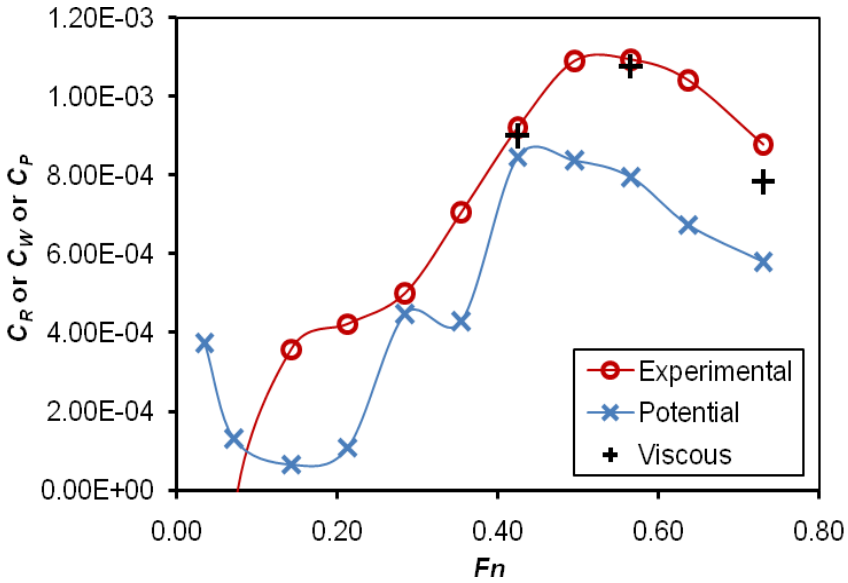

Figure 7 Wave, Pressure and Residual resistance coefficients.

Potential results

In order to validate the use of the non-linear potential solver (5) for the examined type of vessel, systematic numerical tests were conducted for the same speed range as the experiments. The total number of panels used was 12000 while the trim angle as well as the dynamic rise of the

CG, were calculated numerically. The potential results of the examined cases are shown in Table 3. Essentially the method predicts only the wave resistance component C_W, while C_F is derived under the ITTC'57 skin friction approximation. The predicted C_W is compared to the measured one in Fig. 7. Evidently it exhibits the same variations, but it is lower than the experimental in the whole range of Fn. This is an expected behavior according to the aforementioned shortcomings. The potential theory predicts higher waves at the stern region, resulting to increased pressures underneath the stern that in turn leads to a reduction of the total wave resistance. However, the total resistance coefficient appears closer to the experimental in Fig. 6 where the skin friction has been added. This is reflected also to the calculation of the total resistance (which is the meaningful quantity) in Fig. 3, where the calculated results are in satisfactory agreement with the measurements up to the speed of 3.5 m/s (~7%) while deviations increase at higher speeds.

RANS results

In order to explore the possibility of obtaining better results at high speeds with RANS computations, three test cases were examined, corresponding to the speeds of 3, 4 and 5m/s. In any case the grid size had 2.65 million grid points. To reduce the computation cost as well as the uncertainties related with the longitudinal position of the center of gravity, the trim angle of the vessel was taken from the experiments while it was assumed free to heave. The results acquired via the RANS solver are shown in Table 4. First, it is important to notice that the calculated skin friction coefficient C_F is in very good agreement with the empirical ITTC'57 formula in Table 2, which justifies the relevant assumption when the potential method is adopted. The calculated values of the total resistance coefficients are presented in Table 4. Evidently, the total resistance is predicted with satisfactory agreement with respect to the experimental values for the examined speeds. The larger deviation at the highest speed may be a result of the extended wave breaking which was observed during the experiments in this case, which cannot be simulated numerically.

The deviations percent of the calculated vs. the experimental total resistance is depicted in Table 5 for both methods, where the superiority of the RANS approach is obvious at high speeds.

The calculated wave patterns about the boat by the RANS computations are plotted in Figs. 8 to 10 for the speeds of 3.0 m/s, 4.0 m/s and 5.0 m/s, respectively. The full lines represent wave crests while the dashed lines correspond to wave troughs. These plots show a regular formation which is similar to the real one observed during the experiments.

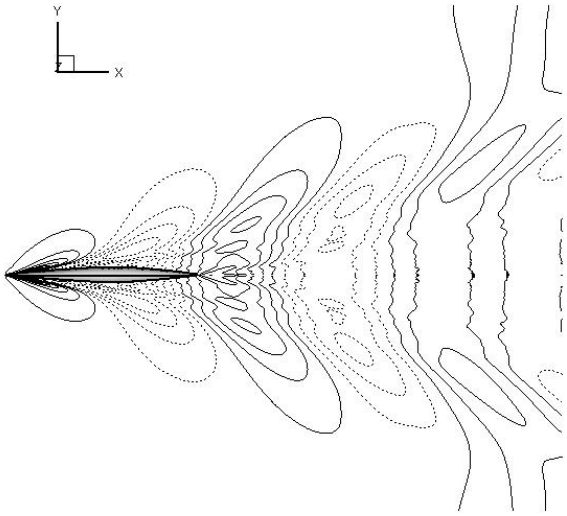

Figure 8 Water surface elevation contour, RANS solver, V_s =2.995 m/s.

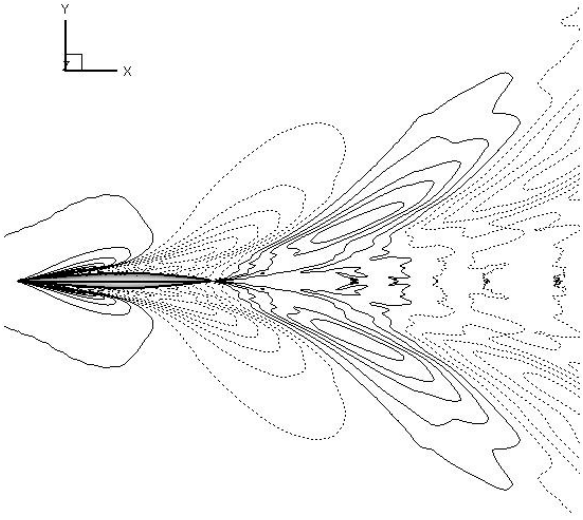

Figure 9 Water surface elevation contour, RANS solver, V_s =3.989 m/s.

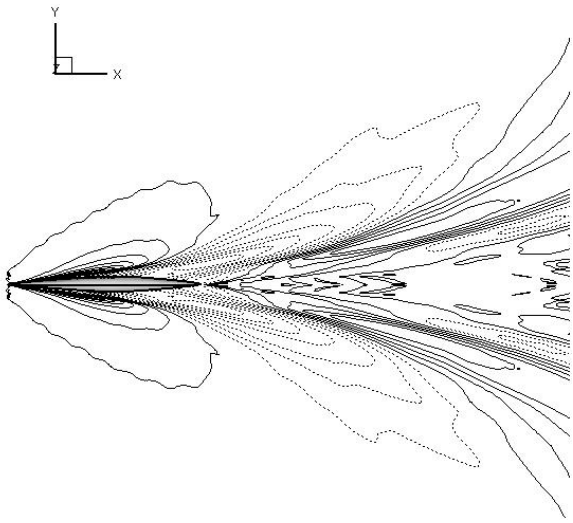

Figure 10 Water surface elevation contour, RANS solver, V_S=5.153 m/s.

Experimental tests in regular waves

The tests in regular waves were done at the speed of 2.5 m/s for wave frequencies of 0.3 Hz, 0.5 Hz, 0.7 Hz and 0.9 Hz and at the speed of 5.0 m/s for wave frequencies of 0.3 Hz and 0.5 Hz (3).

During the tests, the following responses were measured:

C.G. rise

Pitch

Added resistance

Wave Height

The experimental results for these tests are presented in Table 6. Based on the recorded time histories of the boat responses, the Response Amplitude Operators (RAOs) in heave (at the CG position) and in pitch motion were calculated and presented also in this Table, together with the measured values of wave amplitude and mean added resistance.

The non-dimensional RAO values were calculated using the following formulae:

$RAOHEAVE = \xi_0 / \zeta_0$

$RAOPITCH = \theta / (k\ \xi_0)$

Where: ξ_0 : heave response amplitude

ζ_0 : wave amplitude

θ : pitch amplitude [rad]

k : wave number ($k=2\pi/\lambda$)

λ : wave length

The most important result is the resistance increase presented in the last column of Table 6. It can be concluded that the added resistance is negligible for wave lengths much larger than the boat length (low frequency range, examined frequency 0.3 Hz) and can reach values from 7 to 12% for faster waves (examined frequencies 0.5, 0.7 and 0.9 Hz) and for both wave heights. This resistance increase reflects directly to the required power by the athlete.

DISCUSSION

In the previous chapters the results of hydrodynamic resistance tests and numerical calculations performed in the Laboratory for Ship and Marine Hydrodynamics of NTUA on a "Kayak K-1" boat have been presented. The towing resistance as well as the dynamic heave and pitch values were measured for a wide of the speeds, starting from low values and covering the range of interest for the particular boat. The measured total resistance coefficient shows a minimum about the vessel speed of 1.5m/s and a maximum at 3.0 m/s. These values appear as a result of the interactions of the generated wave systems about the boat. In addition, the Froude decomposition of the total resistance coefficient demonstrates that skin friction is higher than the residuary component at all speeds, while at low speeds the appearance of laminar flow regions about the bow is rather possible. Wave breaking has been also observed at speeds above 3.5 m/s.

The performance of the boat subjected to low amplitude heading harmonic waves was also investigated. The main conclusion is that short waves (high frequencies) may increase the boat resistance and, therefore, the required human power by almost 10%.

The applications of the employed CFD approaches have shown that the computation of the total resistance by applying a non-linear potential flow code in conjunction with the ITTC'57 skin friction formula is in good agreement with the measured one for speeds up to 3.5 m/s. Above this level, viscous effects are dominant and RANS methods have to be employed to obtain accurate results. However, in the usual range of speeds of the particular vessel, the potential approach may produce reliable results and, therefore, can be involved in optimization procedures concerning the hull geometry.

The data acquired during this experimental work can form a basis for further investigation and deeper understanding of the athlete-boat interaction, especially for high performance and high competitive boats, like the case at hand.

CONCLUSIONS

The systematic numerical experiments have shown that both potential and RANS methods can be applied in order to calculate the calm water resistance of a flat water racing kayak. The potential solver provided results in good qualitative agreement with the experiments and, therefore, can be involved in optimization procedures concerning the hull geometry. The RANS solver gave very accurate predictions for the total resistance and therefore can be used with confidence for predicting the resistance of vessels of similar geometry.

APPLICATIONS IN SPORT

Within the last years we have a tremendous raise of new technologies (construction materials, e.g. carbon fiber) which in their way affect the increasing improvement of results in canoe - kayak. The main factor for the accomplishment of better times in canoeing is the hydrodynamic resistance of the boat's hull. With this study, every coach may form the way his athlete paddles, taking into consideration the hydrodynamic resistance which is observed depending on the waves appearing during a canoe – kayak race.

Additionally, this study is very important for the canoe – kayak boat manufacturers, since they can achieve making more improved boat hulls, taking into account the hydrodynamic resistance appearing under different types of waves.

ACKNOWLEDGMENTS

The authors wish to thank the personnel of LSMH and particularly Mr. I. Trachanas who has carried out the measurements in the Towing Tank as well as Mr. D. Triperinas, Ms. D. Damala and Mr. G Katsaounis for designing the experiments and interpreting the results.

The authors' would also like to thank Lloyd's Register Educational Trust (LRET), since Mr. Polyzos' Phd studies are supported by LRET.

The Lloyd's Register Educational Trust (LRET) is an independent charity working to achieve advances in transportation, science, engineering and technology education, training and research worldwide for the benefit of all.

REFERENCES

1. Launder, B. E., Spalding, D. B. (1974). The numerical computation of turbulent flows. *Computer Methods in Applied Mechanics and Engineering*, 3, 269-289.

2. Newman, J. N. (1997). Marine Hydrodynamics. Cambridge, Massachusetts and London England: The MIT press, ISBN 0-262-14026-8.

3. Triperinas, D. V., Damala, D., Katsaounis, G. (2009) Report No. NAL 303 F 2009, Laboratory for Ship and Marine Hydrodynamics, NTUA.

4. Tzabiras, G. D. (2004). Resistance and Self-propulsion simulations for a Series-60, CB=0.6 hull at model and full scale. *Ship Technology Research*, 51, 21-34.

5. Tzabiras, G. D. (2008). A method for predicting the influence of an additive bulb on ship resistance. *Proceedings of the 8th International Conference on Hydrodynamics*, 53-60.

6. Tzabiras, G. D., Kontogiannis, K. (2010). An integrated method for predicting the hydrodynamic resistance of low-Cb ships. *Computer-Aided Design Journal,* Accepted for publication.

FIGURES

1.

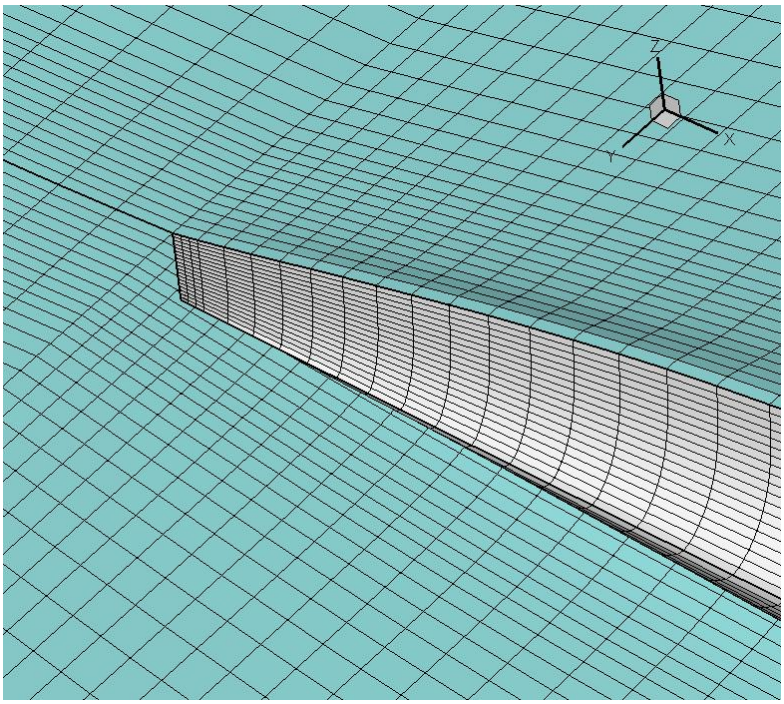

2.

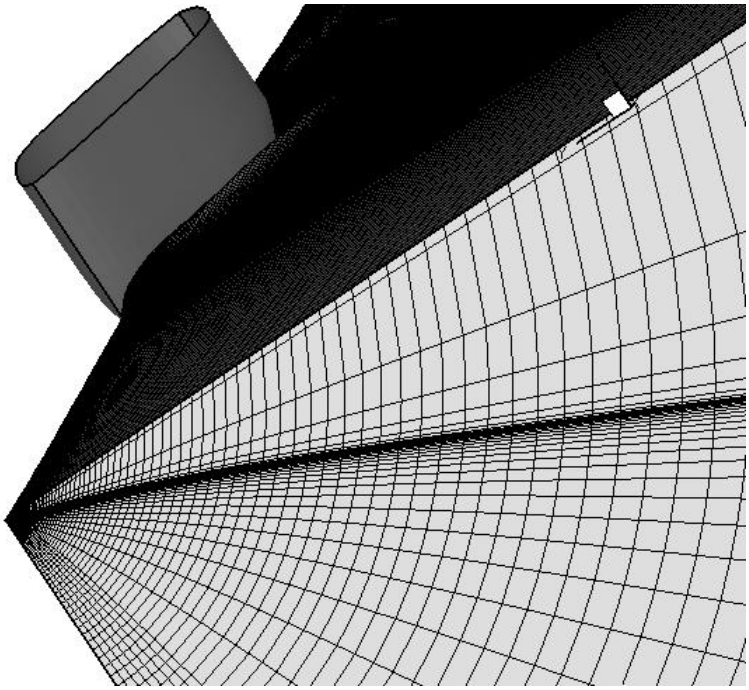

3.

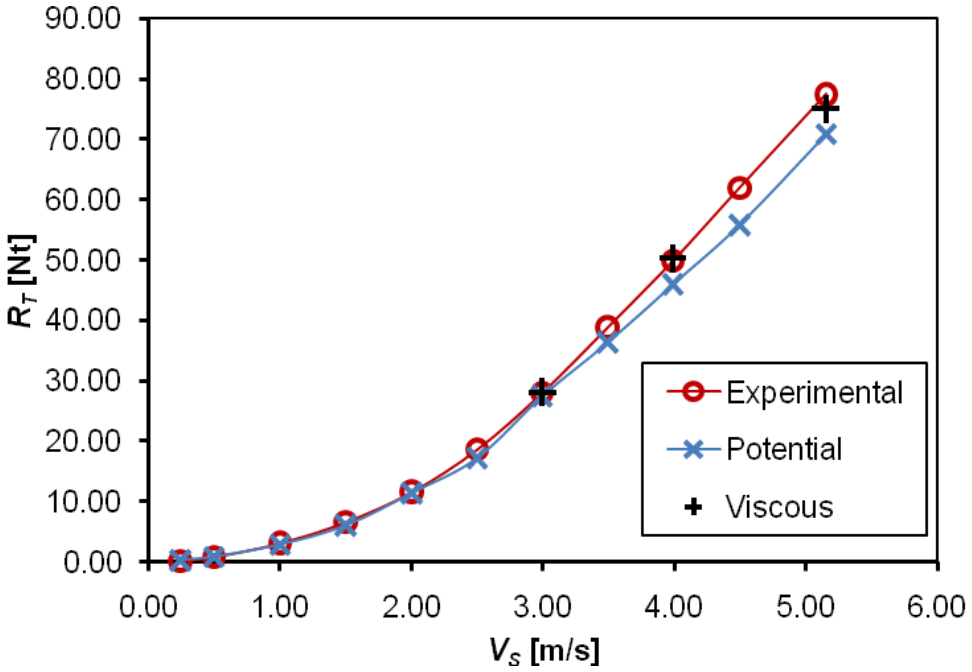
90.00
80.00
70.00
60.00
50.00
40.00
30.00
20.00
10.00
0.00
R_T [Nt]
0.00
1.00
2.00
3.00
4.00
5.00
6.00
V_S [m/s]
Experimental
Potential
Viscous

4.

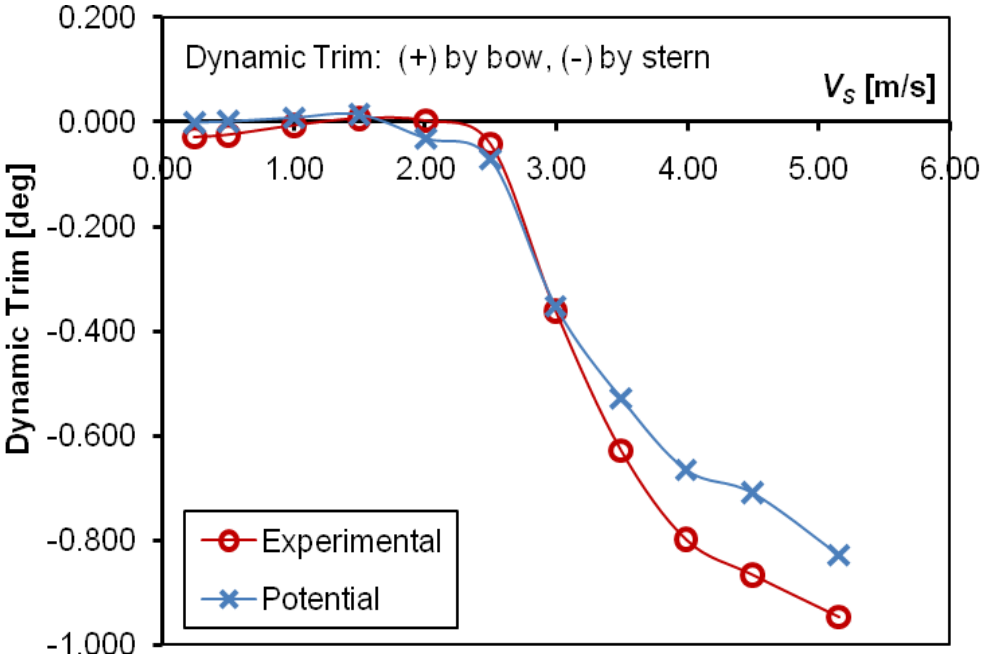
Dynamic Trim: (+) by bow, (-) by stern
V_S [m/s]
0.200
0.000
-0.200
-0.400
-0.600
-0.800
-1.000
Dynamic Trim [deg]
0.00
1.00
2.00
3.00
4.00
5.00
6.00
Experimental
Potential

5.

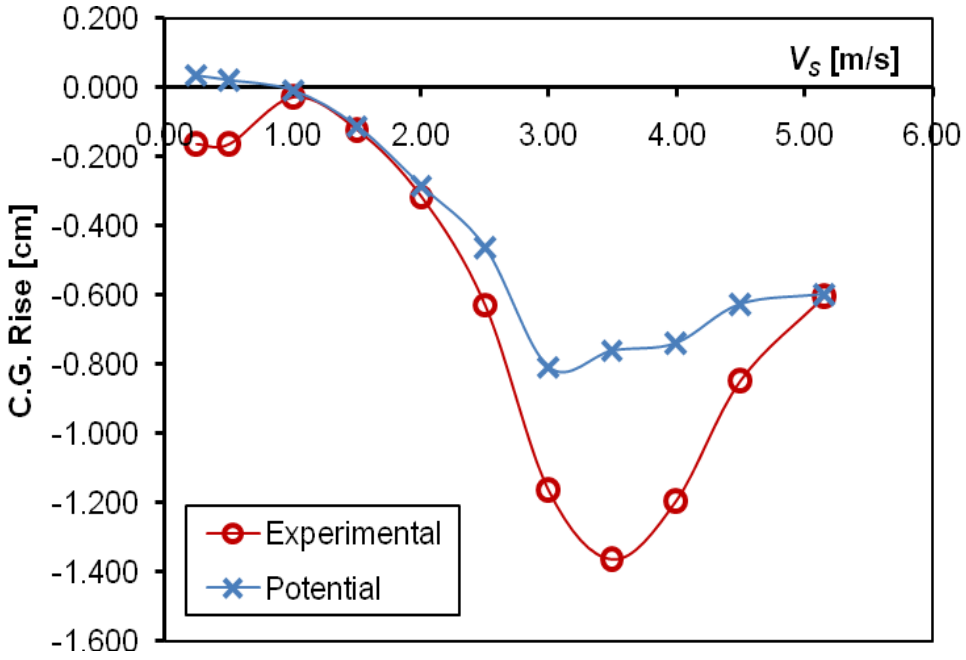
0.200
0.000
-0.200
-0.400
-0.600
-0.800
-1.000
-1.200
-1.400
-1.600
0.00
1.00
2.00
3.00
4.00
5.00
6.00
V_S [m/s]
C.G. Rise [cm]
Experimental
Potential

6.

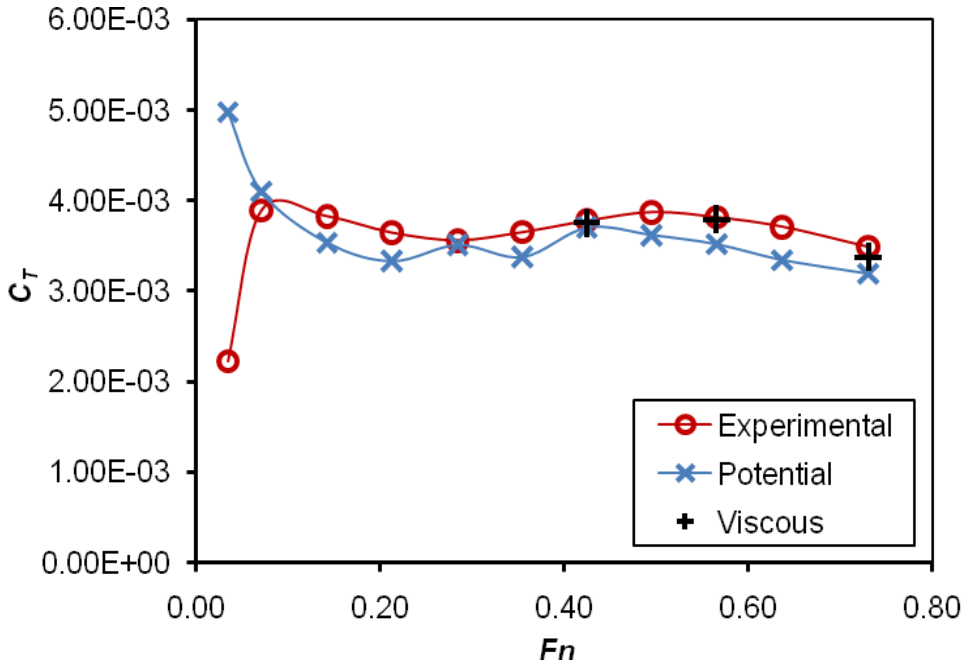
6.00E-03
5.00E-03
4.00E-03
3.00E-03
2.00E-03
1.00E-03
0.00E+00
0.00
0.20
0.40
0.60
0.80
C_T
Fn
Experimental
Potential
Viscous

7.

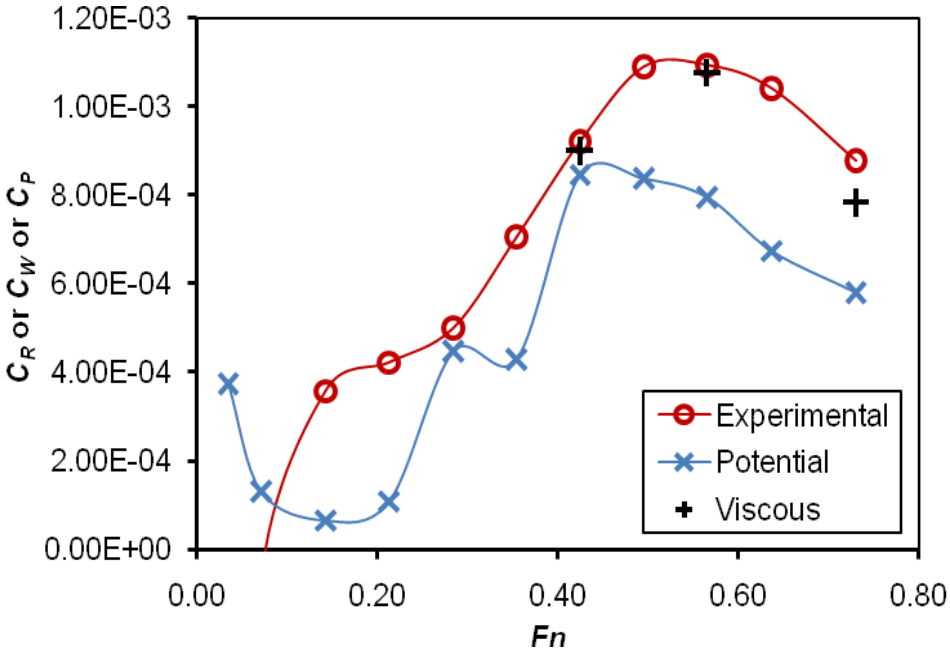
1.20E-03
1.00E-03
8.00E-04
6.00E-04
4.00E-04
2.00E-04
0.00E+00
C_R or C_W or C_P
0.00
0.20
0.40
0.60
0.80
Fn
Experimental
Potential
Viscous

8.

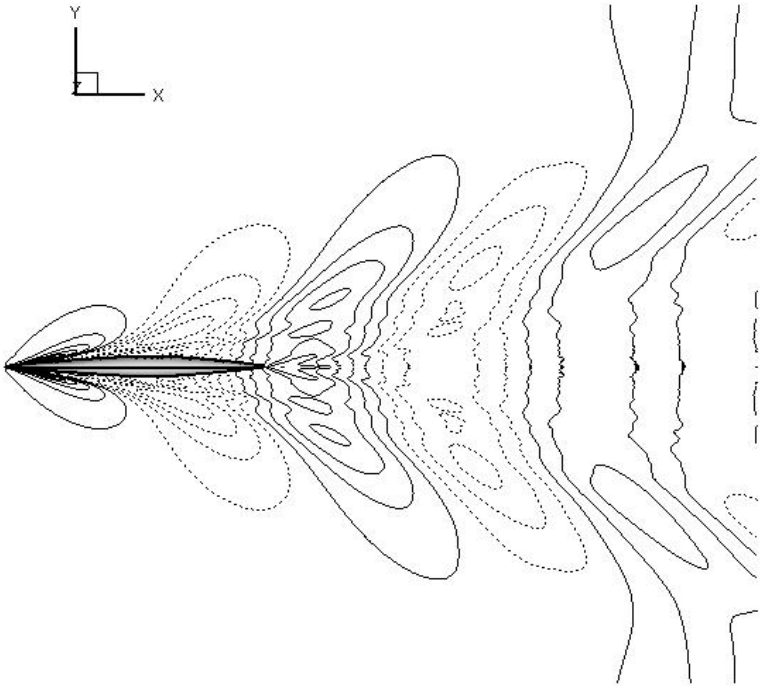
Y
X

9.

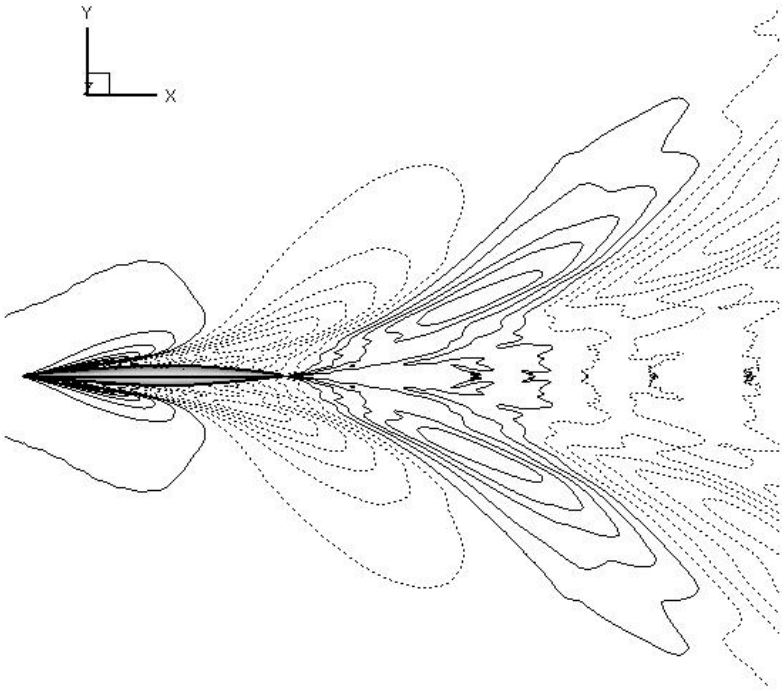

10.

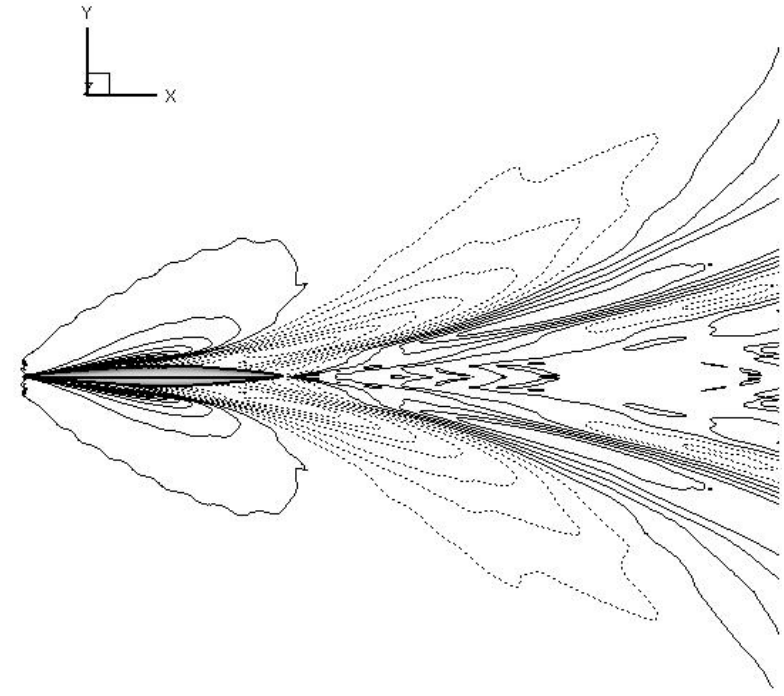

Figure 1 Panels on the hull and water surface.

Figure 2 RANS numerical grid

Figure 3 Total Resistance.

Figure 4 Dynamic Trim.

Figure 5 C.G. Rise.

Figure 6 Total resistance coefficient.

Figure 7 Wave, Pressure and Residual resistance coefficients.

Figure 8 Water surface elevation contour, RANS solver, V_S =2.995 m/s.

Figure 9 Water surface elevation contour, RANS solver, V_S =3.989 m/s.

Figure 10 Water surface elevation contour, RANS solver, V_S=5.153 m/s.

TABLES

TABLE 1 Experimental results for the calm water resistance tests, condition: Δ=86.8 Kp.

Speed m/s	Froude Number	Total Resistance (R_T) Kp	Dynamic Trim (+) by bow, (-) by stern deg	C.G. Rise cm
0.244	0.035	0.011	-0.029	-0.163
0.499	0.071	0.078	-0.025	-0.163
1.003	0.142	0.311	-0.007	-0.027
1.502	0.213	0.669	0.007	-0.122
2.005	0.284	1.179	0.002	-0.317
2.500	0.354	1.896	-0.043	-0.629
2.995	0.425	2.854	-0.361	-1.163
3.493	0.495	3.963	-0.628	-1.362
3.989	0.565	5.085	-0.799	-1.195
4.494	0.637	6.318	-0.866	-0.846
5.153	0.730	7.902	-0.947	-0.602

TABLE 2 Experimental results for the calm water resistance tests

Speed m/s	Froude Number	Total Resistance (R_T) Nt	Total Resistance Coefficient (C_T)	Frictional Resistance Coefficient (C_F) (ITTC'57)	Residual Resistance Coefficient (C_R)
0.244	0.035	0.105	2.226E-03	4.606E-03	-2.380E-03
0.499	0.071	0.761	3.889E-03	3.971E-03	-8.194E-05
1.003	0.142	3.054	3.827E-03	3.470E-03	3.568E-04
1.502	0.213	6.556	3.644E-03	3.222E-03	4.216E-04
2.005	0.284	11.558	3.561E-03	3.061E-03	4.997E-04
2.500	0.354	18.588	3.651E-03	2.946E-03	7.050E-04

2.995	0.425	27.988	3.776E-03	2.856E-03	9.200E-04
3.493	0.495	38.862	3.872E-03	2.783E-03	1.089E-03
3.989	0.565	49.867	3.815E-03	2.722E-03	1.093E-03
4.494	0.637	61.952	3.710E-03	2.670E-03	1.040E-03
5.153	0.730	77.487	3.488E-03	2.611E-03	8.770E-04

TABLE 3 Numerical results for the calm water resistance tests, potential method,

Speed m/s	Froude Number	Dynamic Trim (+) by bow, (-) by stern deg	C.G. Rise cm	Wave Resistance Coefficient (C_W)	Frictional Resistance Coefficient (C_F) (ITTC'57)	Total Resistance Coefficient (C_T)	Total Resistance (R_T) Nt
0.244	0.035	-0.001	0.036	3.743E-04	4.606E-03	4.980E-03	0.235
0.499	0.071	0.001	0.022	1.305E-04	3.971E-03	4.102E-03	0.802
1.003	0.142	0.008	-0.008	6.468E-05	3.470E-03	3.535E-03	2.821
1.502	0.213	0.014	-0.112	1.079E-04	3.222E-03	3.330E-03	5.991
2.005	0.284	-0.032	-0.285	4.473E-04	3.061E-03	3.508E-03	11.388
2.500	0.354	-0.072	-0.462	4.288E-04	2.946E-03	3.375E-03	17.182
2.995	0.425	-0.352	-0.808	8.456E-04	2.856E-03	3.702E-03	27.437
3.493	0.495	-0.528	-0.761	8.367E-04	2.783E-03	3.620E-03	36.330
3.989	0.565	-0.665	-0.739	7.948E-04	2.722E-03	3.517E-03	45.974
4.494	0.637	-0.709	-0.626	6.733E-04	2.670E-03	3.343E-03	55.825
5.153	0.730	-0.828	-0.597	5.797E-04	2.611E-03	3.190E-03	70.881

TABLE 4 Numerical results for the calm water resistance tests, RANS method.

Speed m/s	Froude Number	Pressure Resistance Coefficient (C_P)	Frictional Resistance Coefficient (C_F)	Total Resistance Coefficient (C_T)	Total Resistance (R_T) Nt
2.995	0.425	9.001E-04	2.852E-03	3.752E-03	28.118
3.989	0.565	1.076E-03	2.717E-03	3.792E-03	50.266
5.153	0.730	7.825E-04	2.594E-03	3.376E-03	75.084

TABLE 5 Experimental results for the calm water resistance tests

Speed m/s	Froude Number	Deviation in Total Resistance δR_T (%)	
		Potential	RANS
0.244	0.035	-123.76	-
0.499	0.071	-5.46	-
1.003	0.142	7.63	-
1.502	0.213	8.61	-
2.005	0.284	1.47	-

2.500	0.354	7.56	-
2.995	0.425	1.97	-0.46
3.493	0.495	6.52	-
3.989	0.565	7.81	-0.80
4.494	0.637	9.89	-
5.153	0.730	8.52	3.10

TABLE 6 Experimental results for the tests in regular waves,

Speed	Wave frequency	Wave Amplitude	RAO Heave	RAO Pitch	Added Resistance	Resistance increase
m/s	Hz	cm			Kp	%
2.5	0.3	5.9	0.936	1.111	0.016	0.8
2.5	0.5	5.3	0.565	0.598	0.157	8.3
2.5	0.7	5.3	0.139	0.053	0.132	7.0
2.5	0.9	4.8	0.042	0.018	0.221	11.7
5.0	0.3	5.8	1.045	1.164	0.139	1.9
5.0	0.5	5.2	1.000	0.780	0.873	11.6